Novel branched Nod factor structure results from a-(1-3) fucosyl transferase activity: the major lipo-chitin oligosaccharides from Mesorhizobium loti strain NZP2213 bear an a-(1-3) fucosyl substituent on a nonterminal backbone residue

Olsthoorn, M.M.A.; López-Lara, I.M.; Petersen, B.O.; Bock, K.; Haverkamp, J.; Spaink, H.P.; Thomas-Oates, J.E.

Novel Branched Nod Factor Structure Results from α-(1→3) Fucosyl Transferase Activity: The Major Lipo-Chitin Oligosaccharides from *Mesorhizobium loti* Strain NZP2213 Bear an α-(1→3) Fucosyl Substituent on a Nonterminal Backbone Residue[†]

Maurien M. A. Olsthoorn,[‡] Isabel M. López-Lara,[§,||] Bent O. Petersen,[⊥] Klaus Bock,[⊥] Johan Haverkamp,[‡] Herman P. Spaink,[§] and Jane E. Thomas-Oates*[,‡]

Department of Mass Spectrometry, Bijvoet Center for Biomolecular Research, Faculty of Chemistry, Utrecht University, Sorbonnelaan 16, NL-3584 CA Utrecht, The Netherlands, Institute of Molecular Plant Sciences, Clusius Laboratory, Leiden University, NL-2333 AL Leiden, The Netherlands, and Department of Chemistry, Carlsberg Laboratory, DK-2500 Valby, Denmark

Received December 2, 1997; Revised Manuscript Received March 26, 1998

ABSTRACT: *Mesorhizobium loti* has been described as a microsymbiont of plants of the genus *Lotus*. Lipo-chitin oligosaccharides (LCOs), or Nod factors, produced by several representative *M. loti* strains all have similar structures. Using fast-atom-bombardment tandem mass spectrometry and NMR spectroscopy, we have now examined the LCOs from the type strain NZP2213 and observed a much greater variety of structures than has been described for the strains of *M. loti* studied previously. Interestingly, we have identified as the major LCO a structure that bears a fucose residue α-1,3-linked to the GlcNAc residue proximal to the nonreducing terminal GlcNAc residue. This is the first time, to our knowledge, that substitution on an internal GlcNAc residue of the LCO backbone has been observed. This novel LCO structure suggests the presence of a novel fucosyltransferase activity in strain NZP2213. Since the presence of this extra structure does not have the effect of broadening the host range, we suggest that the modification of the LCOs with a fucose residue linked to a nonterminal GlcNAc residue might provide protection against degradation by a particular host plant enzyme (e.g., a chitinase) or alternatively represents adaptation to a particular host-specific receptor. The action of the α-(1→3) fucosyltransferase seems to reduce significantly the activity of NodS, the methyltransferase involved in the addition of the *N*-methyl substituent to the nonreducing terminal GlcNAc residue. An additional novel LCO structure has been identified having only a $GlcNAc_2$ backbone. This is to our knowledge the first description of such a minimal LCO structure.

The symbiosis between rhizobial bacteria and leguminous plants, resulting in the formation of nitrogen-fixing root nodules, is a species-specific process that is mediated by signal molecules from both the plant and the bacterium. Flavonoids secreted by the host plant induce the transcription of nodulation genes in the bacterium. Many of these gene products are involved in the biosynthesis of lipo-chitin oligosaccharides (LCOs),[1] or Nod factors, that are secreted by the bacterium.

LCOs consist of an oligosaccharide backbone of three to six β-1,4-linked *N*-acetyl-D-glucosamine (GlcNAc) residues. A fatty acid group is attached to the nitrogen of the nonreducing terminal residue. The nature of the fatty acyl chain, the number of GlcNAc residues, and the presence or absence of extra substituents, together determine the host specificity of the bacterium. Species-specific substituents have, to date, only been identified attached to the reducing and the nonreducing terminal residues of the LCO, but not to internal backbone residues (*1*).

Mesorhizobium loti (formerly called *Rhizobium loti*) has been described as a microsymbiont of plants of the genus *Lotus* (*2*). *Lotus* plants are nodulated by *M. loti*, but not by most other rhizobial bacteria, suggesting that *M. loti* produces specific LCO signals. The structural identification of LCOs from several representative *M. loti* strains has been carried out (*3*). The LCOs produced by the different strains all have similar structures, consisting of GlcNAc pentasaccharides

[†] The work was supported by The Netherlands Foundation for Chemical Research (SON) with financial aid from The Netherlands Organization for the Advancement of Pure Research (NWO). H.P.S. was supported by an NWO pionier grant.

* To whom correspondence should be addressed. Fax: +31-30-2518219. E-mail: J.Thomas-Oates@ams.chem.ruu.nl.

[‡] Utrecht University.

[§] Leiden University.

[||] Present address: Institute of Biotechnology, Technical University Berlin, D-13353 Berlin, Germany.

[⊥] Carlsberg Laboratory.

[1] Abbreviations: Cb, carbamoyl group; COSY, correlated spectroscopy; CID, collision-induced dissociation; FAB-MS, fast-atom-bombardment mass spectrometry; GC/MS, gas chromatography−mass spectrometry; GlcNAc, *N*-acetylglucosamine; HexNAc, *N*-acetylhexosamine; HPLC, high-performance liquid chromatography; HSQC, heteronuclear single quantum coherence spectroscopy; LCO, lipo-chitin oligosaccharide; MS/MS, tandem mass spectrometry; NMR, nuclear magnetic resonance; NOESY, nuclear Overhauser enhancement spectroscopy; PMAA, partially methylated alditol acetate; TLC, thin-layer chromatography; TOCSY, total correlation spectroscopy.

S0006-2960(97)02937-1 CCC: $15.00
Published on Web 05/30/1998

($GlcNAc_5$) of which the nonreducing residue is N-methylated and N-acylated with *cis*-vaccenic acid ($C_{18:1}$) or stearic acid ($C_{18:0}$) and, in most cases, also carbamoylated. The major class of *M. loti* LCOs is substituted on C-6 of the reducing terminal residue with a 4-*O*-acetylfucose residue. This fucose residue which was shown to be a major host-specific determinant for nodulation is transferred to the chitin backbone by the fucosyltransferase NodZ (*4*).

Further to our studies of LCOs from *M. loti* and to complete the overview of *M. loti* structures, we have examined the LCOs from wild-type strain NZP2213, which has been described as a type strain by Scott et al. (*5*). Surprisingly, the LCOs from this strain are quite different from those from all other *M. loti* strains studied. We have identified as the major LCO a structure that bears an additional fucose residue attached to a nonterminal GlcNAc residue. This is the first time, to our knowledge, that substitution of an internal GlcNAc residue has been demonstrated in an LCO. This novel LCO structure suggests the presence of a novel fucosyltransferase activity in strain NZP2213. In addition, a further novel LCO structure has been identified having only a $GlcNAc_2$ backbone. To date only backbones composed of three to six GlcNAc residues have been described (*1*) making the novel $GlcNAc_2$ LCO the smallest LCO structure described.

EXPERIMENTAL PROCEDURES

Bacteria, Growth Conditions, and LCO Isolation. Strain *M. loti* NZP2213 was obtained from the DSIR culture collection (Palmerston North, NZ). To achieve LCO production after induction with naringenin the plasmid pMP2112 containing the *R. leguminosarum* biovar *trifolii nodD* gene was introduced into the wild-type strain NZP2213 of *M. loti* (*3*). The construction of plasmid pMP2112 was described previously (*3*), and it was mobilized from *E. coli* to *M. loti* using pRK2013 as a helper plasmid (*6*).

Bacteria for large-scale isolation were grown at 28 °C in 1 L of B^- medium (*7*) containing spectinomycin (400 μg/L) and phosphate buffer (1 mM, pH 7.4). LCOs were produced overnight after addition of naringenin (1 mg/L) as inducer to the culture. LCOs were extracted from the culture with *n*-butanol (300 mL/L) and dried. The samples were redissolved in acetonitrile/water (3:2, v/v) overnight, purified over an octadodecyl silica column (Baker, 1 mg of sorbent), and subsequently submitted to HPLC on a Pep-S column (5 μm, 5 × 250 mm, Pharmacia). Elution was performed with a stepwise gradient of mixtures of acetonitrile and water (highest grade, Baker) (30% acetonitrile for 30 min, 40% for 20 min, 42% for 20 min, 50% for 20 min, 60% for 10 min, and 80% for 15 min) at a flow of 1 mL/min and monitored with an RSD 2140 photodiode array detector (Pharmacia). The HPLC fractions were collected and dried. This procedure was repeated using 3 L of B^- medium to obtain enough material for a detailed NMR analysis.

TLC Analysis. LCOs were radiolabeled by growing 3 mL of bacterial cultures ($OD_{620} = 0.1$) overnight at 15 °C in the presence of 0.4 μCi [1-^{14}C]D-glucosamine (specific activity 50 mCi/mmol, Amersham) together with naringenin (1 μg/mL). After addition of 2 mL of water-saturated *n*-butanol and boiling for 10 min, LCOs were isolated from the cultures by extraction. The extracts were dried and redissolved in 30 μL of water-saturated *n*-butanol. TLC analyses were carried out using normal-phase Silica 60 plates (Aldrich) developed with butanol/ethanol/water (5:3:2, v/v) and reversed-phase C_{18}-coated silica plates (Merck) developed with acetonitrile:water (1:1, v/v). Five microliters of each extract was used for each TLC analysis. Radioactivity was detected using a phosphorimaging system (Molecular Dynamics Co.) that uses ImageQuant software.

Composition Analysis, Linkage Analysis, and Chemical Modifications. Composition analysis (methanolysis followed by re-N-acetylation and trimethylsilylation) yielding trimethylsilyl (TMS) methyl glycosides and linkage analysis (permethylation, hydrolysis, reduction, and *O*-acetylation) yielding partially methylated alditol acetates (PMAAs) were carried out as described (*3*). Mild base de-esterification of approximately one-third of HPLC fractions 1, 3, and 9 (3 L) was carried out in 250 μL of methanol and 250 μL of ammonium hydroxide solution (25% NH_3 in water) overnight at ambient temperature followed by drying.

Mass Spectrometric Analysis. Positive ion mode fast-atom-bombardment mass spectrometry (FAB-MS) was carried out using the first two sectors of a JEOL JMS-SX/SX 102A tandem mass spectrometer operating at 10 kV (mass range *m*/*z* 200−2000) accelerating voltage. The FAB gun was operated at 6 kV accelerating voltage with an emission current of 10 mA using xenon as the bombarding gas. Spectra were scanned at a speed of 30 s for the full mass range specified by the accelerating voltage used and were recorded and processed on a Hewlett-Packard HP 9000 data system. Tandem mass spectra were obtained following collision-induced dissociation (CID) in the third field free region using the same instrument under similar conditions with air as collision gas at a pressure sufficient to reduce the parent ion to half of its original intensity. The probe was loaded with 1 μL of sample solution into a matrix of thioglycerol (2−3 μL). A matrix of thioglycerol saturated with sodium iodide was used for generating $[M + Na]^+$ ions. HPLC fractions were redissolved in 30−300 μL of dimethyl sulfoxide prior to MS analysis.

Gas chromatography−mass spectrometry (GC/MS) was performed using a Fisons MD 800 mass spectrometer fitted with an Interscience 8000 gas chromatograph using a DB-5MS column (0.25 mm × 30 m, J&W Scientific) and an on-column injector, with helium as the carrier gas. PMAAs were separated using the following temperature program: 50 °C for 2 min, a gradient of 40 °C/min to 130 °C, 130 °C for 2 min, a gradient of 4 °C/min to 230 °C, and finally 230 °C for 2 min. Mass spectra were obtained under conditions of electron impact in the positive ion mode and were recorded by linear scanning of the mass range *m*/*z* 55−400 at an ionization potential of 70 eV. TMS methyl glycosides were separated using the following temperature program: 70 °C for 2 min, a gradient of 30 °C/min to 170 °C, 170 °C for 2 min, a gradient of 4 °C/min to 240 °C, and finally 240 °C for 10 min.

NMR Analysis. Spectra were recorded in 5 mm tubes at 750.04 MHz for ^{1}H and at 188.6 MHz for ^{13}C at 310 K using a solution of 200−250 μg of LCOs (isolated as HPLC fractions 7 and 8 from the 3 L culture) in a mixture of acetonitrile-d_6 and D_2O (5:7, v/v) using a Varian UNITY INOVA 750 spectrometer. The chemical shifts are given relative to acetonitrile (1.95 ppm) for ^{1}H and (1.3 ppm) for ^{13}C. The

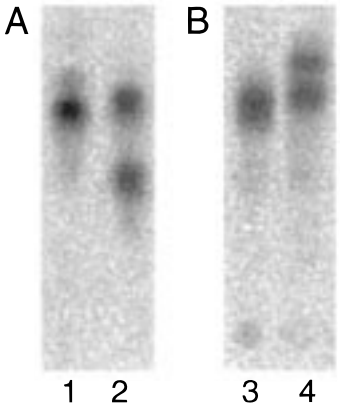

FIGURE 1: TLC profiles of radiolabeled LCOs from *M. loti* E1R (lanes 1 and 3) and NZP2213 (lanes 2 and 4) (A) normal-phase and (B) reversed-phase.

amount of sample used for NMR analysis was estimated using HPLC with UV detection at 206 nm and comparing the peak area obtained with that obtained from a known amount of standard, analyzed under similar conditions.

The double-quantum-filtered phase-sensitive correlated spectroscopy (COSY) experiment was performed using the Varian standard program TNDQCOSY (*8*, *9*), with 0.340 s acquisition time and 4K data points. Data in the F1 dimension were zero filled to give a matrix of 4K × 2K points, and all data points were resolution enhanced in both dimensions by a shifted sine-bell function. Nuclear Overhauser enhancement spectroscopy (NOESY) experiments were performed using the Varian standard program TNNOESY (*10*), with a mixing time of 200 ms. Total correlation spectroscopy (TOCSY) experiments were performed using the Varian standard program TNTOCSY (*11*, *12*), with a spin-lock time of 120 ms. Heteronuclear single quantum coherence spectroscopy (HSQC) experiments were performed using the pulse field gradient standard Varian program GHSQC (*13*), with a gradient strength of 4, 4, and 2 G/cm, respectively, and gradient time of 2.0, 2.0 and 0.5 ms, respectively. Spectra were assigned using the computer program PRONTO (*14*), which allows a simultaneous display of different 2D spectra and individual labeling of the cross-peaks.

A GESA/Monte Carlo simulation of a hexasaccharide having a structure similar to that of the LCO in fractions 7 and 8, but having *N*-acetyl groups on all glucosamine residues, was carried out using the approach published recently for fucosylated trisaccharides (*15*).

RESULTS

TLC Analysis of Lipo-Chitin Oligosaccharides. The structure of the LCOs from the different *M. loti* strains studied to date (*3*) all appear to be very similar. The complete structures of the LCOs from E1R.pMP2112 have been described (*3*) and are used for comparison purposes in this study. In an initial screen, the behavior of the LCOs produced by *M. loti* strain E1R.pMP2112 were compared with the behavior of those from strain NZP2213.pMP2112 on both normal- and reversed-phase TLC plates. LCOs were radiolabeled by growing the bacteria in the presence of [1-^{14}C]D-glucosamine after induction with naringenin. The TLC profiles (Figure 1) show a clear difference in the migration behavior of the LCOs produced by the two strains. While the normal-phase chromatogram (Figure 1A) of LCOs from strain E1R bears one major spot (lane 1), that for the LCOs from strain NZP2213 contains two spots (lane 2). The first has an R_f value comparable although not identical with the spot observed for strain E1R. The second intense spot migrates more slowly than the first, and we thus conclude that it corresponds to a more hydrophilic LCO component. A similar phenomenon is observed for the reversed-phase chromatogram (Figure 1B), which bears one major spot (lane 3) for LCOs from strain E1R, while that for LCOs from strain NZP2213 contains two (lane 4). The second spot for the LCOs from NZP2213 migrates faster than the broad spot for the LCOs from E1R, indicating that it corresponds to LCOs that are more hydrophilic than those from E1R. To determine the structures of the LCOs corresponding to these new TLC spots, large-scale isolation of the LCOs from NZP2213 was carried out, followed by HPLC separation and analysis using MS and NMR.

HPLC Separation and Mass Spectrometric Analysis. Two separate cultures (1 and 3 L) of *M. loti* NZP2213 were grown in the presence of naringenin in order to obtain enough material for a detailed NMR analysis. The LCOs from both cultures were extracted with *n*-butanol, and after prepurification on C_{18} solid-phase cartridges they were partially separated using HPLC. The HPLC profile obtained from the extract of the 3 L culture (Figure 2) has a series of peaks eluting between 40 and 50% acetonitrile in water. Nine HPLC fractions (Figure 2) were collected and analyzed using positive ion mode FAB-MS (Table 1). The fractions are mixtures since only a crude fractionation of LCOs was obtained using HPLC. Identical LCO profiles were detected from the two cultures.

Interestingly, the *m*/*z* values for the major $[M + H]^+$ pseudomolecular ions (Table 1) corresponding to LCOs produced by NZP2213 are not the same as those for the LCOs produced by all other strains of *M. loti* analyzed, but instead correspond to analogues consisting of two, three, four, or five GlcNAc residues bearing a carbamoyl group (Cb) and an *O*-acetylfucose residue but, in addition, bearing an extra deoxyhexose residue and, in general, lacking the methyl group. Surprisingly, while a large variety of novel LCO structures is produced by the type strain, structures corresponding to those identified from all other *M. loti* strains are present only as minor components or are totally absent. In addition to the major species bearing $C_{18:1}$ and $C_{18:0}$ fatty acyl chains, components bearing $C_{16:1}$, $C_{16:0}$, OH-$C_{18:1}$ (hydroxyl fatty acid), $C_{20:1}$, $C_{20:0}$, and $C_{22:1}$ fatty acyl substituents were also identified. It has been described that adduct ions form between compounds containing unsaturated fatty acid groups and the thioglycerol matrix used for the FAB-MS analysis (*17*). This phenomenon was used to confirm the assignment of species having unsaturated fatty acyl chains.

The pseudomolecular ions for the major LCO components in the most intense HPLC peaks (fractions 3−8) were submitted to tandem mass spectrometric analysis in order to determine the arrangement of substituents and to identify the site of attachment of the nonacetylated deoxyhexose residue. The CID mass spectrum (Figure 3) of the pseudomolecular ion for one of the major LCOs from *M. loti* NZP2213 (fraction 7) at *m*/*z* 1635 contains a series of oxonium or B-ions (*18*) at *m*/*z* 1226, 1023, 820, and 471 which arise from cleavage of each successive glycosidic

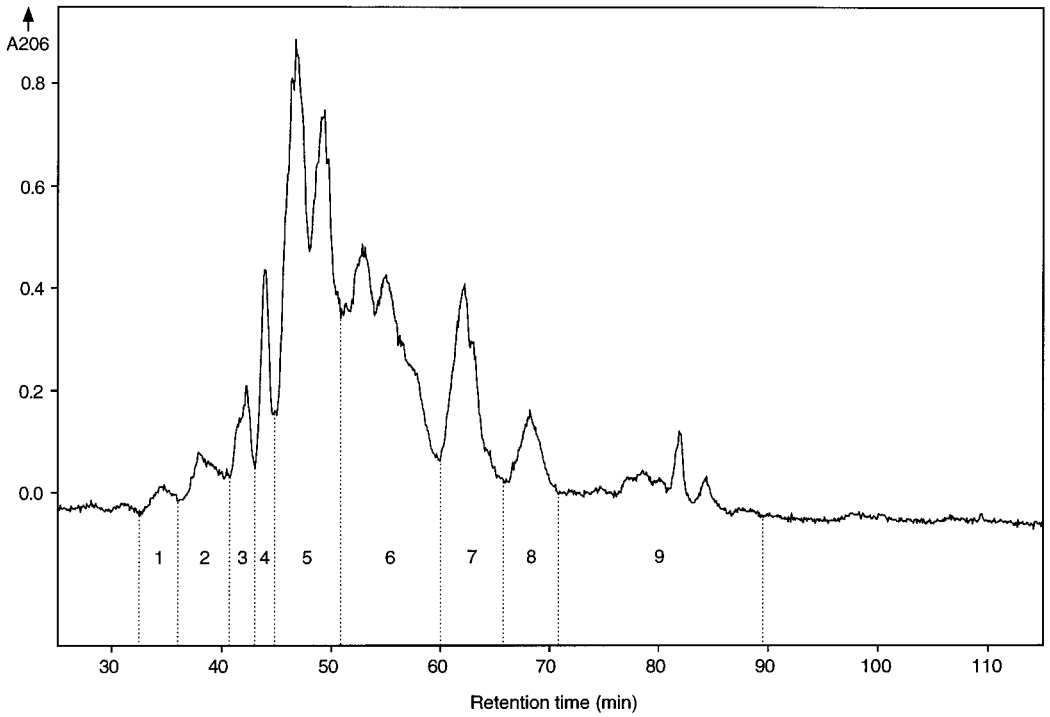

FIGURE 2: HPLC profile of *n*-butanol extract of 3 L culture from *M. loti* NZP2213 (absorbance at 206 nm). Fractions collected are indicated.

Table 1: Summary of LCO Structures[a] from *M. loti* NZP2213

LCO structure[b]	[M + H]$^+$	HPLC fraction no. (3 L)	additional analyses
V($C_{20:1}$,Cb,Ac,AcFuc,Fuc)	1703	9	-Ac[c]
V($C_{22:1}$,Cb,AcFuc,Fuc)	1689	9	MS/MS
V($C_{20:0}$,Cb,AcFuc,Fuc)	1663	9	MS/MS
V($C_{20:1}$,Cb,AcFuc,Fuc)	**1661**	**8, 9**	**MS/MS,NMR, -Ac**
V($C_{18:0}$,Me,Cb,AcFuc,Fuc)	1649	9	MS/MS, -Ac
V(OH−$C_{18:1}$,Cb,AcFuc,Fuc)	1649	3	MS/MS, -Ac
V($C_{18:0}$,Cb,AcFuc,Fuc)	**1635**	**7, 8**	**MS/MS,NMR**
V($C_{18:1}$,Cb,AcFuc,Fuc)	**1633**	**5, 6**	**MS/MS**
V($C_{16:1}$,Me,Cb,AcFuc,Fuc)	1619	3	MS/MS, -Ac
V($C_{16:0}$,Cb,AcFuc,Fuc)	**1607**	**3, 4**	**MS/MS, -Ac**
V($C_{16:1}$,Cb,AcFuc,Fuc)	1605	1, 2	-Ac
V($C_{18:0}$,Cb,Fuc,Fuc)	1593	6	MS/MS
V($C_{18:1}$,Cb,Fuc,Fuc)	**1591**	**4, 5**	**MS/MS**
V($C_{16:0}$,Cb,Fuc,Fuc)	**1565**	**3, 4**	**MS/MS, -Ac**
V($C_{18:0}$,Me,Cb,AcFuc)	1503	9	MS/MS, -Ac
V($C_{18:1}$,Me,Cb,AcFuc)	1501	6	
V($C_{18:1}$,Cb,AcFuc)	1487	5−7	MS/MS
V($C_{20:1}$,Me,Cb,Fuc)	1487	9	MS/MS, -Ac
V($C_{20:1}$,AcFuc)	1472	9	-Ac
V($C_{16:1}$,Cb,AcFuc)	1459	1−3	MS/MS, -Ac
V($C_{18:1}$,AcFuc)	1444	5	
V($C_{16:0}$,Me,Fuc)	1390	7, 8	
V($C_{16:1}$,Me,Fuc)	1388	5	
IV($C_{18:0}$,Me,Cb,AcFuc)	1300	9	-Ac
IV($C_{20:0}$,Cb,Fuc)	1272	9	
IV($C_{20:1}$,Cb,Fuc)	1270	8, 9	-Ac
IV($C_{18:0}$,Me,Cb,Fuc)	1258	9	-Ac
IV($C_{18:0}$,Cb,Fuc)	1244	8, 9	-Ac
IV($C_{18:1}$,Cb,Fuc)	1242	6	MS/MS
III($C_{18:0}$,Cb,Fuc)	1041	9	MS/MS, -Ac
II($C_{18:1}$,Cb)	690	9	-Ac

[a] Major components are given in bold. [b] Nomenclature (substituents listed clockwise starting from fatty acid) (*16*). [c] Mild base deesterification.

bond, as shown in the fragmentation scheme. These fragments indicate that the LCO is composed of a linear backbone of five GlcNAc residues bearing a carbamoyl group and a $C_{18:0}$ fatty acyl group on the nonreducing terminal residue, an acetyldeoxyhexose on the reducing terminal residue, and a deoxyhexose residue on the internal GlcNAc residue proximal to the nonreducing terminal GlcNAc residue (see Figure 3). In addition, ions arising by loss of a deoxyhexose residue (146 mass units) by β-cleavage are observed from all oxonium ions except for from the B_1-ion at *m*/*z* 471, consistent with this assignment (Figure 3). It is curious to note that, while the deoxyhexose residue is readily cleaved under CID conditions, fragment ions arising by similar cleavage of the acetyldeoxyhexose residue are absent.

To exclude the formal possibility that some of the fragment ions in the above spectrum could arise as the result of internal residue loss (*19*, *20*), deoxyhexose migration (*21*), or isomerization of long-lived ions prior to fragmentation (*22*), the [M + Na]$^+$ pseudomolecular ion of one of the major components at *m*/*z* 1655 was subjected to CID-MS, since it has been postulated that rearrangement processes such as internal residue loss do not occur from [M + Na]$^+$ parent ions.[2] The fragment ions present in the CID mass spectrum (not shown) arise unambiguously from the structure proposed, in which the nonacetylated deoxyhexosyl substituent is attached to the GlcNAc residue proximal to the nonreducing terminus.

CID experiments carried out on other [M + H]$^+$ pseudomolecular ions at *m*/*z* 1689 (fraction 9), 1663 (fraction 9), 1661 (fractions 8 and 9), 1649 (fractions 3 and 9), 1633 (fractions 5 and 6), 1619 (fraction 3), 1607 (fractions 3 and 4), 1593 (fraction 6), 1591 (fractions 4 and 5), and 1565 (fractions 3 and 4), all corresponding to species containing two deoxyhexose residues (see Table 1), were carried out and yielded similar results, demonstrating that the major LCO components from *M. loti* NZP2213 all bear an extra nonacetylated deoxyhexose residue on the GlcNAc residue proximal to the nonreducing terminal GlcNAc residue.

[2] L. P. Brüll, V. Kovácik, J. Haverkamp, W. Heerma, and J. E. Thomas-Oates, Unpublished observations.

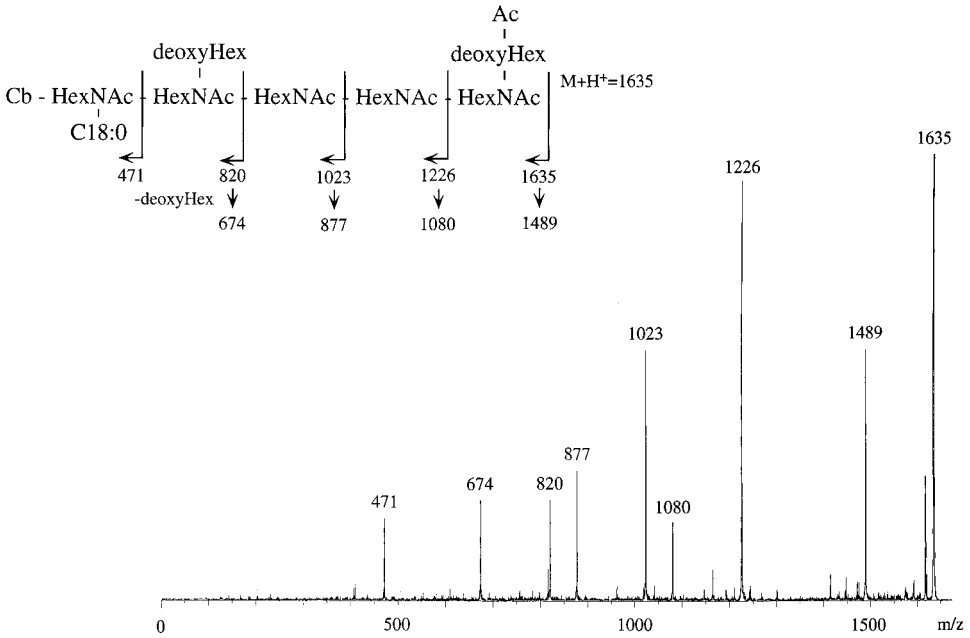

FIGURE 3: CID tandem mass spectrum obtained from one of the major LCO components V($C_{18:0}$,Cb,AcFuc,Fuc) on collision of *m*/*z* 1635 from HPLC fraction 7 of *M. loti* NZP2213.

Additional $[M + H]^+$ pseudomolecular ions were detected (fractions 6, 8, and 9) at *m*/*z* 1300, 1272, 1270, 1258, 1244, and 1242 consistent with LCOs consisting of $GlcNAc_4$ and $GlcNAc_3$ backbones bearing a deoxyhexose or an acetyldeoxyhexose residue (Table 1). Prior to this study, only LCOs containing a $GlcNAc_5$ backbone have been observed from *M. loti*. To determine the position of the deoxyhexose residue on the GlcNAc backbone, CID experiments were performed on the $[M + H]^+$ and on the $[M + Na]^+$ ions. The CID mass spectra (not shown) revealed a series of fragment ions that allowed the site of attachment of the deoxyhexose residue to be determined unambiguously as the reducing GlcNAc residue.

Surprisingly, in HPLC fraction 9 a novel LCO was identified having a $GlcNAc_2$ backbone, which is, to our knowledge, the smallest LCO structure described. The ion at *m*/*z* 690 corresponding to this novel LCO II($C_{18:1}$,Cb) is intense enough to also be accompanied by its structurally diagnostic B_1-ion at *m*/*z* 469. This small LCO structure is unlikely to result from chemical or enzymatic fragmentation on storage of the HPLC fractions, since its late HPLC elution position (in fraction 9) is consistent with the existence of such a hydrophobic species in the original LCO extract.

Because some HPLC fractions represent a very complex mixture of components that are not always present in quantities sufficient to allow CID experiments to be carried out, additional structural information from LCOs in fractions 1, 3, and 9 was obtained using mild base de-esterification (see Table 1), which selectively removes *O*-acetyl groups. The mass spectrometric shifts were used to determine the number of *O*-acetyl groups present in the different LCOs and to confirm the proposed structures. The results allow us to establish the number of *O*-acetyl groups in a minor LCO whose pseudomolecular ion is observed in the mass spectrum of HPLC fraction 9 at *m*/*z* 1703 and which had been proposed to represent a species corresponding to V($C_{20:1}$,Cb,Ac,AcDeoxyHex,DeoxyHex). In the mass spectrum (not shown) of the HPLC fraction after mild base de-esterification, the pseudomolecular ion is shifted by 84 mass units to *m*/*z* 1619, consistent with the removal of two *O*-acetyl groups and thus confirming the proposed structure in which one *O*-acetyl group is attached to a deoxyhexose residue while the other *O*-acetyl group is attached to the GlcNAc backbone. This is the first demonstration of an *O*-acetyl group attached to the GlcNAc backbone in LCOs from *M. loti*.

Composition and Linkage Analysis. Composition analysis (data not shown) was performed on the HPLC fractions derived from the 1 L of culture that contains LCOs bearing two deoxyhexose residues to determine the identity of the deoxyhexose residues. GC/MS analysis of the resulting TMS methyl glycosides, together with those from authentic fucose and rhamnose standards, demonstrated that the only deoxyhexose residue in the LCO-containing fractions from *M. loti* NZP2213 is fucose.

To determine the linkage of the fucose residues to the GlcNAc backbone, linkage analysis (data not shown) was carried out on those HPLC fractions derived from the 1 L of culture that contains LCOs bearing two fucose residues. GC/MS analysis of the PMAAs indicated the presence of derivatives corresponding to terminal HexNAc, 4-substituted HexNAc, 3,4-substituted HexNAc, 4,6-substituted HexNAc, and terminal deoxyhexose. These results show that one fucose residue is linked 1→3 and the other 1→6 to the 1→4 linked chitin backbone. By analogy with the LCO structures identified from other *M. loti* strains, we suggest that the 4-*O*-acetylfucose residue is linked 1→6 to the reducing terminal GlcNAc residue and that, therefore, the nonacetylated fucose residue is linked 1→3 to the GlcNAc residue proximal to the nonreducing terminal GlcNAc residue.

NMR Analysis. HPLC fractions 7 and 8 (Figure 2) containing the major LCOs bearing two fucose residues and differing only in their fatty acyl substituents (see Table 1) were pooled and further subjected to NMR analyses in order to confirm the linkages and sites of attachment of the fucose residues and to determine the anomericity of the linkages,

Table 2: ^{1}H NMR Chemical Shifts (ppm), Coupling Constants (Hz), and ^{13}C NMR Chemical Shifts (ppm) for LCOs in Fractions 7 and 8 from *M. loti* NZP2213[a]

residue	H-1 ($J_{1,2}$) C-1	H-2 ($J_{2,3}$) C-2	NAc	H-3 ($J_{3,4}$) C-3	H-4 ($J_{4,5}$) C-4	H-5 C-5	H-6 ($J_{5,6}$) C-6	H-6′ ($J_{5,6'}$) ($J_{6,6'}$)
β-GlcNAc−(1→4) (**A**)	4.508	3.753		4.63	3.27	3.38	3.500	3.831
	(8)	(10)		(10)	(9)	75.7	(6)	(3)
	101.5	53.6		75.7	69.2		61.6	(12)
α-Fuc-(1→3) (**B**)	4.98	3.588		3.79	3.663	4.58	1.15	
	(4)	(10)		69.6	72.1	66.6	(6.5)	
	98.9	68.0					15.3	
→3,4)-β-GlcNAc−(1→4) (**C**)	4.44	3.825	1.93[b]	3.72	3.81	3.37	3.636	3.76
	(8)	(10)	21.9	75.2	73.6	75.7	(6)	(4)
	101.6	55.6					60.0	(12)
→4)-β-GlcNAc−(1→4) (**D**)	4.43	3.644	1.92[b]	3.56	3.45	3.41	3.501	3.70
	(8)	(10)	21.9	72.4	79.7	74.8	(6)	(4)
	101.6	54.9					60.3	(12)
→4)-β-GlcNAc−(1→4) (**E**)	4.506	3.65	1.92[b]	3.57	3.482	3.42	3.52	3.712
	(8)	(10)	21.9	72.4	79.8	74.8	(6)	(3)
	101.5	55.9					60.3	(12)
α-Fuc-(1→6) (**F**[c])	4.76	3.67		3.753	3.659	3.99	1.11	
	(4)	(10)		69.7	72.1	66.7	(6.5)	
	99.7	68.5					15.1	
α-Fuc-(1→6) (**F**[d])	4.77					3.96	1.10	
→4,6)-α-GlcNAc (**G**)	5.03	3.78	1.94[b]	3.708	3.62	3.86	3.58	3.707
	90.8	54.0	21.9	69.5	(10)	69.3	(5)	(2)
					79.9		67.1	(12)
→4,6)-β-GlcNAc (**G**)	4.53	3.568	1.97[b]	3.53	3.591	3.488		
	95.5	55.3	21.9		79.9	73.8		
fatty acid (N-2) C20:1	0.82	1.24		1.28	1.97	5.33		
C18:0	0.82	1.24		1.20	2.09			
	12.6	29.4		29.4	35.9			

[a] Recorded in acetonitrile-d_6/D_2O (5:7,v/v) at 37 °C; reference acetonitrile ^{1}H, 1.95 ppm; ^{13}C, 1.3 ppm. [b] May be reversed. [c] Linked to β-GlcNAc (**G**). [d] Linked to α-GlcNAc (**G**).

as well as the linkage positions of the acetyl and carbamoyl groups.

The ^{1}H NMR data (750 MHz) obtained at 310 K from a solution of fractions 7 and 8 in acetonitrile-d_6/D_2O (5:7,v/v) (*3*) are presented in Table 2 and the spectrum is shown in Figure 4. The assignments for the anomeric protons (Figure 4) are based on phase-sensitive double-quantum-filtered COSY, TOCSY, and HSQC experiments, together with NOESY experiments. The *J* values (hertz ± 0.5) (Table 2) are only given for the anomeric and neighboring protons to verify the assignments of the anomeric configurations of the individual monosaccharide residues (**A**−**G**, see Figure 5 for labeling of residues). The ^{13}C NMR data (188.6 MHz) are also given in Table 2 and are based on 2D HSQC spectra and therefore only include signals for protonated carbon atoms. Spatial contacts determined using 2D NOESY experiments are presented in Table 3 and confirm the structural identities using intra-residue NOE contacts together with the spectral assignments. The specific interactions classified as strong, medium, or weak (Table 3) are based on a qualitative evaluation of the intensities of the individual cross-peaks. The results of a molecular dynamics simulation are shown in Figure 6 with labeling of the short distances (average values from the Monte Carlo simulation) between protons based on the experimentally detected NOE contacts (Table 3).

The spectral data were recorded in acetonitrile-d_6/D_2O (5:7, v/v). However, attempts were first made to obtain the spectra in DMSO-d_6 solution, but the lines were too broad to allow assignment of signals. These experiments, however, indicated that the 6-linked fucose **F** had lost 70% of its *O*-4 acetyl group. The chemical shifts for the 4-*O*-acetylated fucose residue in DMSO-d_6 are as follows: 4.75 ppm (H-1), 3.58 ppm (H-2), 3.78 ppm (H-3), 5.03 ppm (H-4), 4.04 ppm (H-5), 0.95 ppm (H-6), and 2.06 ppm (*O*-acetyl), respectively. These data clearly indicate that the 4-position is substituted with an electronegative substituent.

Analysis of the NMR data allows us to propose the LCO structure given in Figure 5 for the components in fractions 7 and 8. Signals for the now unsubstituted fucose **F** are doubled due to the anomeric mixture present in this solvent of the mutarotating reducing GlcNAc **G**; the shifts are consistent with those of a 6-linked fucose residue. The downfield shift of H-3 (4.63 ppm) of the nonreducing GlcNAc **A** is consistent with carbamoyl substitution of *O*-3. The chemical shifts for GlcNAc **D** and **E** are consistent with shifts for 4-linked GlcNAc oligomers (*23*). Finally, the chemical shift for the second fucose **B** (H-1 at 4.98 ppm) clearly indicates that it is attached to a secondary alcohol group on GlcNAc **C**. A strong NOE contact is observed between the H-1 of fucose **B** and H-3 of GlcNAc **C**. Furthermore, H-5 of fucose **B** is shifted significantly downfield (at 4.58 ppm as compared to 3.99 ppm in fucose **F**) as a consequence of its three-dimensional structure (*24*). The difference in chemical shifts for GlcNAc **C** compared with those for GlcNAc **D** and **E** is consistent with these observations.

The NOESY data (Table 2) are consistent with the structure proposed (Figure 5); intra-residue NOE contacts (Table 3) are particularly useful in this context. In addition, a complete set of inter-residue NOE contacts between protons attached to the C atoms involved in the glycosidic linkages, for example, that between H-1 of GlcNAc **A** and H-4 of GlcNAc **C** is observed (Table 3), indicative of a 1→4 linkage

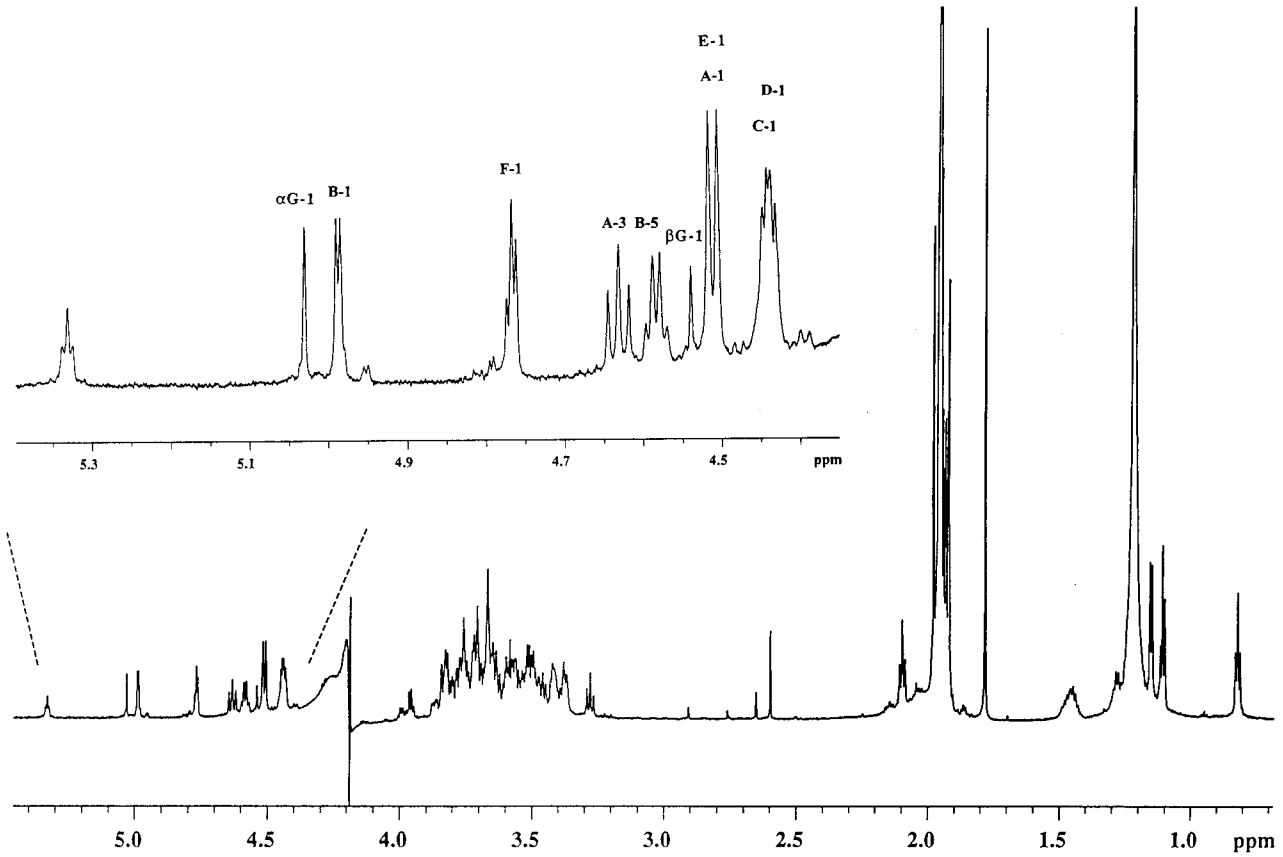

FIGURE 4: ^{1}H NMR spectrum of pooled HPLC fractions 7 and 8 of LCOs from *M. loti* NZP2213. See Figure 5 for labeling of residues.

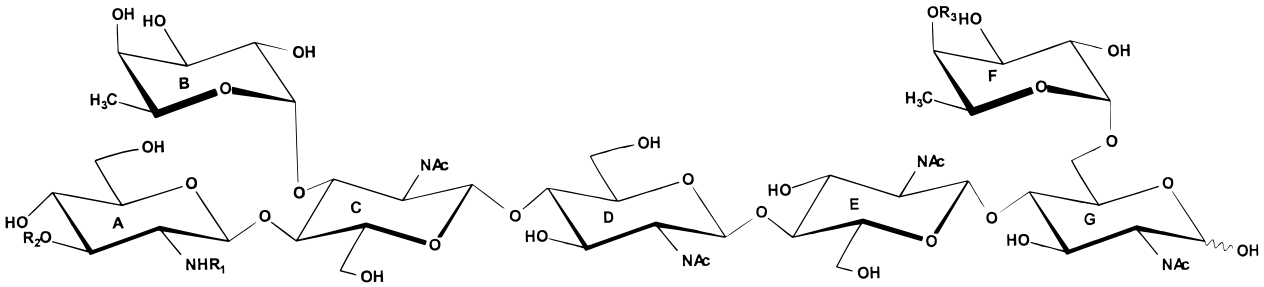

FIGURE 5: Structure of LCOs in the pooled HPLC fractions 7 and 8 of *M. loti* NZP2213. Monosaccharide residues are labeled **A**−**G** as used in Tables 2 and 3 and throughout the text. R_1, predominantly C20:1 and C18:0, with other minor fatty acids; R_2, carbamoyl NH_2CO-; R_3, acetyl or H.

Table 3: NOE Contacts Observed in NOESY Spectrum Obtained from LCOs in Fractions 7 and 8 from *M. loti* NZP2213[a]

residue	from proton	intra-residual	inter-residual				
β-GlcNAc-(1→4) (**A**)	**A**-1	**A**-2(m)	**A**-3(s)	**A**-5(s)	**C**-4(s)	**C**-6(m)	**C**-6′(w)
α-Fuc-(1→3) (**B**)	**B**-1	**B**-2(s)			**C**-3(s)	**C**-2(w)	
	B-5				**A**-2(w)		
	B-6				**A**-2(w)		
→3,4)-*β*-GlcNAc-(1→4) (**C**)	**C**-1	**C**-2(m)	**C**-3(s)	**C**-5(s)	**D**-4(s)	**D**-6(m)	**D**-6′(w)
→4)-*β*-GlcNAc-(1→4) (**D**)	**D**-1	**D**-2(m)	**D**-3(s)	**D**-5(s)	**E**-4(s)		
→4)-*β*-GlcNAc-(1→4) (**E**)	**E**-1	**E**-2(m)	**E**-3(s)	**E**-5(s)	**G**-4(s)		
α-Fuc-(1→6) (**F**)	**F**-1	**F**-2(s)					
→4,6)-α-GlcNAc (**G**)	**G**-1(m)	**G**-2(m)					
→4,6)-*β*-GlcNAc (**G**)	**G**-1(m)	**G**-2(m)	**G**-3(s)	**G**-5(s)			

[a] (s) strong; (m) medium; (w) weak; based on a qualitative evaluation of the intensity of the NOE cross-peaks.

from GlcNAc **A** to **C**. Furthermore, characteristic long-range NOE contacts between H-5 and H-6 protons in fucose **B** and H-2 in GlcNAc **A**, as recently published for 2-substituted fucose trisaccharides (*15*), are observed, together with NOE contacts between H-1 and H-6 protons of neighboring GlcNAc residues.

Finally, a molecular mechanics calculation of an analogue of fractions 7 and 8 (lacking the *O*-acetyl and *O*-carbamoyl groups and in which the N atoms are all substituted with an acetyl group instead of one bearing a fatty acid group) revealed results that are fully consistent with these experimental observations. Results from this model are consistent

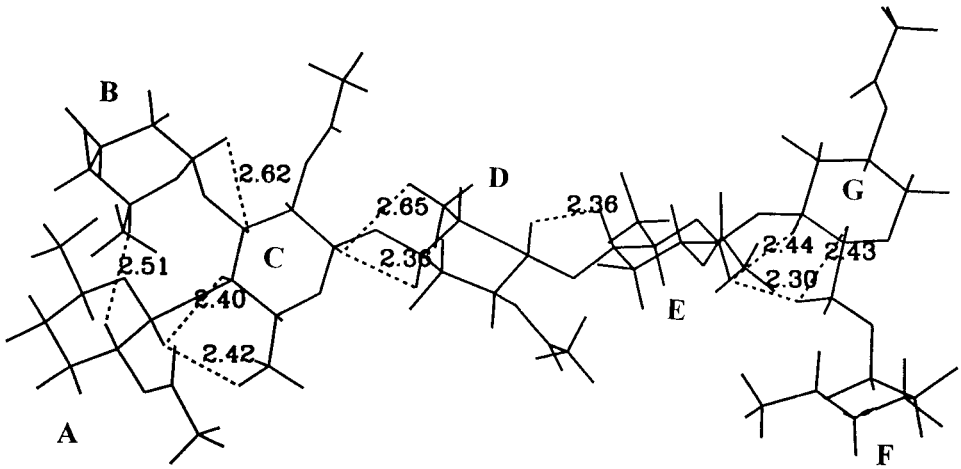

FIGURE 6: Conformation of the LCO oligosaccharide backbone based on Monte Carlo simulation indicating selected, observed interresidue NOE contacts. Average values for the short distances between protons are given.

with results published for a synthetic tetrasaccharide of repeating GlcNAc residues (*23*) with a fatty acid *N*-substituent on the nonreducing terminal residue.

DISCUSSION

Surprisingly, *M. loti* NZP2213 produces a broad profile of LCOs that is quite different from those described for the *M. loti* LCOs analyzed to date. The major LCO components consist of a $GlcNAc_5$ backbone bearing a carbamoyl group and a $C_{16:1}$, $C_{16:0}$, $C_{18:1}$, $C_{18:0}$, $OH-C_{18:1}$, $C_{20:1}$, $C_{20:0}$, or $C_{22:1}$ N-linked fatty acyl chain on the nonreducing terminal GlcNAc residue, bearing a 4-*O*-acetylfucose α-1,6-linked to the reducing terminal GlcNAc residue, and, strikingly, bearing a fucose α-1,3-linked to the GlcNAc residue proximal to the nonreducing terminal residue (see Table 1).

To our knowledge, this is the first time that substitution of the chitin backbone on a nonterminal residue has been observed. Interestingly, these novel LCOs bearing an α-1,3-linked fucose on the GlcNAc residue proximal to the nonreducing terminal residue are the major LCO components produced by the bacterium. LCOs possessing only the 4-*O*-acetylfucosyl substituent on the reducing terminal GlcNAc residue corresponding to those identified from all other *M. loti* strains are observed only as minor components or are absent altogether.

The intense new spots observed in the TLC profiles of LCOs from NZP2213 correspond to radiolabeled LCOs that are more hydrophilic than the *M. loti* LCOs described to date, and we thus assign these spots as corresponding to the LCOs bearing the second fucosyl substituent. The other spots for NZP2213 having comparable although not identical R_f values with the spots for E1R probably correspond to the less hydrophilic LCOs that are substituted by only one fucose residue and are largely different from the *M. loti* LCOs identified to date.

In addition to a $GlcNAc_5$ backbone, LCO components are identified as having a $GlcNAc_4$ or $GlcNAc_3$ backbone, which to date have not been observed from *M. loti*. The only fucose residue present in the shorter LCOs was shown to be attached to the reducing terminal GlcNAc residue, suggesting that the novel fucosyltransferase may only recognize the $GlcNAc_5$ backbone for addition of a second fucosyl substituent. Similarly specific activity has been observed for other *nod* gene products, e.g., NodX in strain TOM of *Rhizobium leguminosarum* biovar *viciae* O-acetylates $GlcNAc_5$ LCOs but not $GlcNAc_4$ LCOs (*25*).

An additional novel LCO structure having only a $GlcNAc_2$ backbone has been identified. To date, such a small LCO structure has not been described, with only backbones composed of three to six GlcNAc residues having been observed (*1*). It is tempting to speculate that such a molecule represents the minimal LCO structure, although it is much more likely, bearing no reducing terminal substituents, to arise as an incomplete biosynthesis product.

Interestingly, the *N*-methyl substituent, present in the LCOs from all other *M. loti* strains studied, is not present in the major LCOs from strain NZP2213, although the minor LCO components that do not bear the extra nonacetylated fucose are methylated in NZP2213. This indicates that the activity of NodS, the methyltransferase involved in the addition of the *N*-methyl substituent to the nonreducing terminal GlcNAc residue, although clearly present in NZP2213, might be significantly reduced by the action of the α-(1→3) fucosyltransferase.

Clearly, NZP2213 produces a greater variety of different LCO structures than the *M. loti* strains analyzed to date. It has been proposed that the great variety of LCOs produced by *Rhizobium* sp. NGR234 explains its broad host range (*26*, *27*). It has been shown that NZP2037, another type strain of *M. loti*, has a broader host range than most *M. loti* strains (*28*) and that its LCOs bear an additional carbamoyl group (*3*). This suggests that the second carbamoyl group might be involved in broadening of the host range. NZP2213, however, forms, together with most other *M. loti* strains, effective, nitrogen-fixing nodules (Nod^+Fix^+) on a limited legume host range (*29*−*31*), suggesting that the novel LCOs found in NZP2213 do not contribute to host range broadening. We thus suggest that the modification of the LCOs with a fucose residue linked to a nonterminal GlcNAc residue might provide protection against degradation by a particular host plant enzyme (e.g., a chitinase), or an adaptation to a particular host-specific receptor.

Furthermore, Mergaert et al. (*32*) have suggested that LCO glycosylations are important for modulating biological activity. *Azorhizobium caulinodans* strain ORS571 produces, as does *M. loti* strain NZP2213, a heterogeneous mixture of

LCOs that are N-methylated and, in general, *O*-carbamoylated on the nonreducing GlcNAc residue. Its LCOs are variably glycosylated on the reducing terminal GlcNAc residue with an arabinose residue (O-3), a fucose residue (O-6), or both. Glycosylated LCOs are more active than unglycosylated LCOs in root hair formation assays on *Sesbania rostrata*. Lorquin et al. (*33*) have suggested that both arabinosylation and fucosylation of LCOs, specifically detected in several unrelated *Sesbania* symbionts are structural requirements for the nodulation of these tropical legumes, underlining the close relationship between LCO structure and host specificity.

To our knowledge, α-(1→3) fucosyltransferase activity has not been identified in Rhizobia to date. In both plant and animal glycoprotein glycans, α-(1→3) fucosyltransferase activities have been described that result in the addition of α-(1→3) fucose to a GlcNAc residue. Many antigenic carbohydrates on the surfaces of cells contain fucose residues α-1,3- or α-1,4-linked to subterminal and/or internal GlcNAc residues. The α-(1→3) fucosyltransferase activity identified in *Rhizobium* seems thus to have a similar activity to that of eukaryotic α-(1→3) fucosyltransferases.

Recently, NodZ, the α-(1→6) fucosyltransferase present in *M. loti* involved in the addition of the fucosyl substituent to C-6 of the reducing terminal GlcNAc residue, has been purified and characterized (*34*). This enzyme seems to be comparable to eukaryotic enzymes that fucosylate the chitobiosyl core of biantennary N-linked glycans in glycoproteins. It is striking that, despite the similarities in activities of the eukaryotic and bacterial α-(1→6) fucosyltransferases, that there is almost no amino acid sequence homology between the two enzymes. It would thus be very interesting to compare the amino acid sequences of our novel *Rhizobium* α-(1→3) fucosyltransferase with those of the known mammalian α-(1→3) fucosyltransferases (*35, 36*). Isolation of enzymatic activity in order to identify and sequence the gene responsible for the α-(1→3) fucosyltransferase activity is therefore a subject of ongoing research.

ACKNOWLEDGMENT

The authors would like to thank the Carlsberg Laboratory for providing temporary accommodation and facilities for M.M.A.O. The authors are grateful to Dr. Jens Ø. Duus for carrying out the molecular dynamics simulation. The 750 MHz NMR spectra were obtained at The Danish National Instrument Center for Biomolecular NMR Spectroscopy.

REFERENCES

1. Dénarié, J., Debellé, F., and Promé, J.-C. (1996) *Annu. Rev. Biochem. 65,* 503−535.
2. Jarvis, B. W., Vanberkum, P., Chen, W. X., Nour, S. M., Fernandez, M. P., Cleyetmarel, J. C., and Gillis, M. (1997) *Int. J. Syst. Bacteriol. 47,* 895−898.
3. López-Lara, I. M., van den Berg, J. D. J., Thomas-Oates, J. E., Glushka, J., Lugtenberg, B. J. J., and Spaink, H. P. (1995) *Mol. Microbiol. 15,* 627−638.
4. López-Lara, I. M., Blok-Tip, L., Quinto, C., Garcia, M. L., Stacey, G., Bloemberg, G. V., Lamers, G. E. M., Lugtenberg, B. J. J., Thomas-Oates, J. E., and Spaink, H. P. (1996) *Mol. Microbiol. 21,* 397−408.
5. Scott, D. B., Young, C. A., Collins-Emerson, J. M., Terzaghi, E. A., Rockman, E. S., Lewis, P. E., and Pankhurst, C. E. (1996) *Mol. Plant-Microbe Interact. 9,* 187−197.
6. Ditta, G., Stanfield, S., Corbin, D., and Helinski, D. R. (1980) *Proc. Natl. Acad. Sci. U.S.A. 77,* 7347−7351.
7. van Brussel, A. A. N., Planqué, K., and Quispel, A. (1977) *J. Gen. Microbiol. 101,* 51−56.
8. Piantini, U., Sørensen, O. W., and Ernst, R. R. (1982) *J. Am. Chem. Soc. 104,* 6800−6801.
9. Rance, M., Sørensen, O. W., Bodenhausen, G., Wagner, G., Ernst, R. R., and Wüthrich, K. (1983) *Biochem. Biophys. Res. Commun. 117,* 479−485.
10. States, D. J., Haberkorn, R. A., and Ruben, D. J. (1982) *J. Magn. Reson. 48,* 286−292.
11. Bax, A., and Davis, D. G. (1985) *J. Magn. Reson. 65,* 355−360.
12. Levitt, M., Freman, R., and Frenkiel, T. (1982) *J. Magn. Reson. 47,* 328−330.
13. Bodenhausen, G., and Ruben, D. J. (1980) *Chem. Phys. Lett. 69,* 185−189.
14. Kjær, M., Andersen, K. V., and Poulsen, F. M. (1994) *Methods Enzymol. 239,* 288−307.
15. Duus, J. Ø., Nifant'ev, N., Shashkov, A. S., Khatuntseva, E. A., and Bock, K. (1996) *Carbohydr. Res. 288,* 25−44.
16. Spaink, H. P. (1992) *Plant Mol. Biol. 20,* 977−986.
17. Fukuda, M. N., Dell, A., Oates, J. E., Wu, P., Klock, J. C., and Fukuda, M. (1985) *J. Biol. Chem. 260,* 1067−1082.
18. Domon, B., and Costello, C. E. (1988) *Glycoconjugate J. 5,* 397−409.
19. Kovácik, V., Hirsch, J., Kovác, P., Heerma, W., Thomas-Oates, J., and Haverkamp, J. (1995) *J. Mass Spectrom. 30,* 949−958.
20. Brüll, L. P., Heerma, W., Thomas-Oates, J., Haverkamp, J., Kovácik, V., and Kovác, P. (1997) *J. Am. Soc. Mass Spectrom. 8,* 43−49.
21. Ernst, B., Müller, D. R., and Richter, W. J. (1997) *Int. J. Mass Spectrom. Ion Processes 160,* 283−290.
22. Ferro, M., Demont, N., Promé, D., Promé, J.-C., Boivin, C., and Dreyfus, D. (1994) *13th International Mass Spectrometry Conference,* Budapest, Poster Th D3.
23. Robina, I., Lopez-Barba, E., Jimenez-Barbero, J., Martin-Pastor, M., and Fuentes, J. (1997) *Tetrahedron: Asymmetry 8,* 1207−1224.
24. Lemieux, R. U., Bock, K., Delbaere, L. T. J., Koto, S., and Rao, V. S. (1980) *Can. J. Chem. 58,* 631−653.
25. Firmin, J. L., Wilson, K. E., Carlson, R. W., Davies, A. E., and Downie, J. A. (1993) *Mol. Microbiol. 10,* 351−360.
26. Price, N. P. J., Relic, B., Talmont, F., Lewin, A., Promé, D., Pueppke, S. G., Maillet, F., Dénarié, J., Promé, J.-C., and Broughton, W. J. (1992) *Mol. Microbiol. 6,* 3575−3584.
27. Price, N. P. J., Talmont, F., Wieruszeski, J.-M., Promé, D., and Promé, J.-C. (1996) *Carbohydr. Res. 289,* 115−136.
28. Scott, D. B., Chua, K. Y., Jarvis, B. D. W., and Pankhurst, C. E. (1985) *Mol. Gen. Genet. 201,* 43−50.
29. Pankhurst, C. E., Craig, A. S., and Jones, W. T. (1979) *J. Exp. Bot. 30,* 1085−1093.
30. Pankhurst, C. E., and Jones, W. T. (1979) *J. Exp. Bot. 30,* 1095−1107.
31. Pankhurst, C. E., Hopcroft, D. H., and Jones, W. T. (1987) *Can. J. Bot. 65,* 2676−2685.
32. Mergaert, P., Ferro, M., D'Haeze, W., van Montagu, M., Holsters, M., and Promé, J.-P. (1997) *Mol. Plant-Microbe Interact. 10,* 683−687.
33. Lorquin, J., Lortet, G., Ferro, M., Méar, N., Dreyfus, B., Promé, J.-C., and Boivin, C. (1997) *Mol. Plant-Microbe Interact. 10,* 879−890.
34. Quinto, C., Wijfjes, A. H. M., Bloemberg, G. V., Blok-Tip, L., López-Lara, I. M., Lugtenberg, B. J. J., Thomas-Oates, J. E., and Spaink, H. P. (1997) *Proc. Natl. Acad. Sci. U.S.A.* 94, 4336−4341.
35. Macher, B. A., Holmes, E. H., Swiedler, S. J., Stults, C. L. M., and Srnka, C. A. (1991) *Glycobiology 1,* 577−584.
36. de Vries, T., and van den Eijnden, D. H. (1992) *Histochem. J. 24,* 761−770.

BI972937R